Archival Report

Biological Psychiatry: Celebrating 50 Years

Connectivity Profile Predictive of Effective Deep Brain Stimulation in Obsessive-Compulsive Disorder

Juan Carlos Baldermann, Corina Melzer, Alexandra Zapf, Sina Kohl, Lars Timmermann, Marc Tittgemeyer, Daniel Huys, Veerle Visser-Vandewalle, Andrea A. Kühn, Andreas Horn, and Jens Kuhn

ABSTRACT

BACKGROUND: Deep brain stimulation for obsessive-compulsive disorder is a rapidly developing treatment strategy for treatment-refractory patients. Both the exact target and impact on distributed brain networks remain a matter of debate. Here, we investigated which regions connected to stimulation sites contribute to clinical improvement effects and whether connectivity is able to predict outcomes.

METHODS: We analyzed 22 patients (13 female) with treatment-refractory obsessive-compulsive disorder undergoing deep brain stimulation targeting the anterior limb of the internal capsule/nucleus accumbens. We calculated stimulation-dependent optimal connectivity separately for patient-specific connectivity data of 10 patients and for 12 additional patients using normative connectivity. Models of optimal connectivity were subsequently used to predict outcome in both an out-of-sample cross-validation and a leave-one-out cross-validation across the whole group.

RESULTS: The resulting models successfully cross-predicted clinical outcomes of the respective other sample, and a leave-one-out cross-validation across the whole group further demonstrated robustness of our findings ($r = .630$, $p < .001$). Specifically, the degree of connectivity between stimulation sites and medial and lateral prefrontal cortices significantly predicted clinical improvement. Finally, we delineated a frontothalamic pathway that is crucial to be modulated for beneficial outcome.

CONCLUSIONS: Specific connectivity profiles, encompassing frontothalamic streamlines, can predict clinical outcome of deep brain stimulation for obsessive-compulsive disorder. After further validation, our findings may be used to guide both deep brain stimulation targeting and programming and to inform noninvasive neuromodulation targets for obsessive-compulsive disorder.

Keywords: Connectome, Deep brain stimulation (DBS), Diffusion magnetic resonance imaging (dMRI), Lead-DBS, Obsessive-compulsive disorder (OCD), Tractography

https://doi.org/10.1016/j.biopsych.2018.12.019

Obsessive-compulsive disorder (OCD) is among the most common neuropsychiatric disorders, with a lifetime prevalence of 2.3% (1). The involvement of altered cortico-striato-thalamo-cortical loops along with a frontostriatal dysfunction is a generally accepted concept in the pathophysiology of OCD (2,3). Despite increasing knowledge about network impairments, there is very limited information about which networks can be modulated to help to improve symptoms in OCD.

Deep brain stimulation (DBS) has been successfully employed to alleviate symptoms in severe treatment-resistant OCD (4). Based on the aforementioned frontostriatal dysfunction model, the ventral striatum, nucleus accumbens (NAC), and nearby anterior limb of the internal capsule (ALIC) have become the most common targets [see (5) for a review]. Response rates show high variability, and to date, reliable predictors for the intervention have not been identified (4). Although the exact mechanism of DBS for OCD remains vague, there is increasing evidence that the stimulation exerts both local and distributed effects on functional brain networks (6). A study based on 11 subjects found that DBS induced a reduction in functional connectivity between the NAC and both medial and lateral prefrontal cortices (PFCs) and that this effect correlated positively with outcome (7). Structural connectivity to the right middle frontal gyrus (MFG) was also identified to be associated with a better clinical response in a sample of 6 patients, whereas connectivity to the orbitofrontal cortex was associated with nonresponse (8). Of note, studies assessing networks associated with DBS for OCD reveal widespread prefrontal structures and are based on small sample sizes. The heterogeneity in identifying corticostriatal pathways that carry out beneficial effects in neuromodulatory treatment for OCD is also reflected by the different cortical targets used for

SEE COMMENTARY ON PAGE 708

ISSN: 0006-3223

transcranial magnetic stimulation, which include the dorsolateral PFC, supplementary motor area, and orbitofrontal cortex [see (9) for a meta-analysis and an overview].

In summary, although it seems certain that DBS has effects on distributed brain networks, it remains highly unclear which networks are associated with clinical improvement. It is, however, vitally important to characterize such therapeutic networks, as they may serve to guide targeting for both invasive and noninvasive brain stimulation (10). In Parkinson's disease (PD), recently a study defined connectivity profiles of effective DBS electrodes (11). Moreover, these profiles were able to robustly predict treatment outcome across cohorts and DBS centers. With similar knowledge in OCD, current neuromodulative treatment could be improved and new stimulation protocols could be developed, thereby increasing effectivity and possibly reducing adverse events.

Here, we aimed at assessing stimulation-dependent connectivity profiles that are associated with and predictive of outcome in DBS for OCD. First, we hypothesized that beneficial effects of DBS are associated with stimulation of a prefrontostriatal network. Second, we hypothesized that stimulation-dependent connectivity profiles would predict individual outcomes of DBS for OCD in out-of-sample data.

METHODS AND MATERIALS

Subjects and Clinical Assessments

A total of 22 patients (13 female) were recruited from the outpatient clinic of the psychiatric department for obsessive-compulsive spectrum disorders at the University Hospital of Cologne in Germany. All patients were diagnosed with severe treatment-refractory OCD, qualifying them for DBS surgery. Definitions of severity and treatment refractoriness are given in the Supplement. Included patients underwent DBS surgery to the ALIC/NAC, receiving two quadripolar DBS electrodes (model 3389 [n = 19] or 3387 [n = 3]; Medtronic, Minneapolis, MN). Preoperative clinical assessments included demographic data and evaluation of symptom severity using the Yale-Brown Obsessive Compulsive Scale (Y-BOCS). Final assessment of symptom severity took place 12 months (±1 month) after surgery when stimulation settings remained stable. All subjects provided written informed consent, and the study was approved by the Ethics Committee of the University of Cologne.

Imaging Acquisition and Preprocessing

For each patient, structural high-resolution, T1-weighted images were acquired on a 3T Philips Healthcare magnetic resonance imaging (MRI) scanner (Philips Medical Systems, Hamburg, Germany) at the University Hospital of Cologne before surgery. Postoperative computer tomography was obtained for each patient after surgery to verify correct electrode placement. A subgroup of 10 patients (8 female) received preoperative diffusion MRI (dMRI) using echo-planar imaging (repetition time = 16800 ms, echo time = 82 ms, field of view = 220 mm, voxel size = 1.7 × 1.7 × 1.7 mm, 90 sampling directions, b value 3000 s/mm^2) on a 3T Siemens Magnetom PRISMA (Siemens Medical Systems, Erlangen, Germany). A detailed description of dMRI data analysis is given in the Supplement.

DBS Lead Localization and Volume of Tissue-Activated Estimation

DBS electrodes were localized using Lead-DBS software (http://www.lead-dbs.org) as described elsewhere (11). Briefly, postoperative computer tomography scans were linearly coregistered to preoperative MRI using Advanced Normalization Tools (12) (http://stnava.github.io/ANTs/). A subcortical refinement step was added to adjust for brain shift that may have occurred during surgery (brain shift correction module in Lead-DBS). Images were then normalized into International Consortium for Brain Mapping 2009b nonlinear asymmetric space using the SyN approach implemented in Advanced Normalization Tools. An additional subcortical refinement step was applied to attain a most precise subcortical alignment between patient and template space. Results were visually reviewed to confirm accuracy. Volumes of tissue activated (VTA) were modeled following the approach described in Horn *et al.* (11). Briefly, the electric field was estimated using a finite element method on a four-compartment mesh describing local gray and white matter as well as electrode contact and insulating material (see Figure 1 for schematic display of methods and Figure 2 for visualization of individual electrode localization).

Connectivity Estimation

For the patient-specific connectivity, a dMRI diffusion scheme implemented in DSI Studio (http://dsi-studio.labsolver.org/) was used analog to the assessment of the normative group connectome (see below). Specifically, diffusion data were reconstructed using generalized q-sampling imaging (13) with a diffusion sampling length ratio of 1.25. The restricted diffusion was quantified using restricted diffusion processing (14). A deterministic fiber tracking algorithm (14) was used, and the angular threshold was 60°. The step size was 0.86 mm. The anisotropy threshold was determined automatically by DSI Studio. Tracts with length below 10 mm were discarded. A total of 200,000 tracts were calculated per subject. The whole-brain fiber set was then normalized into standard stereotactic space following the approach described in Horn *et al.* (15,16) as implemented in Lead-DBS. For normative structural connectivity, a publicly available group connectome was used that is based on multishell diffusion-weighted and T2-weighted imaging data from 32 subjects of the Human Connectome Project at Massachusetts General Hospital [https://ida.loni.usc.edu/ (17)] as described elsewhere (15).

Creating and Validating a Data-Driven Profile of Optimal DBS Connectivity

A data-driven approach to identify networks correlating with the clinical outcome across the sample was applied that has been introduced in the context of PD before (11). Briefly, from the whole-brain connectome estimated for each subject (or the Human Connectome Project normative connectome), fibers running through the VTA were selected and projected to the brain in a weighted fashion. Weighting was performed on a normalized version of the electric field gradient strength

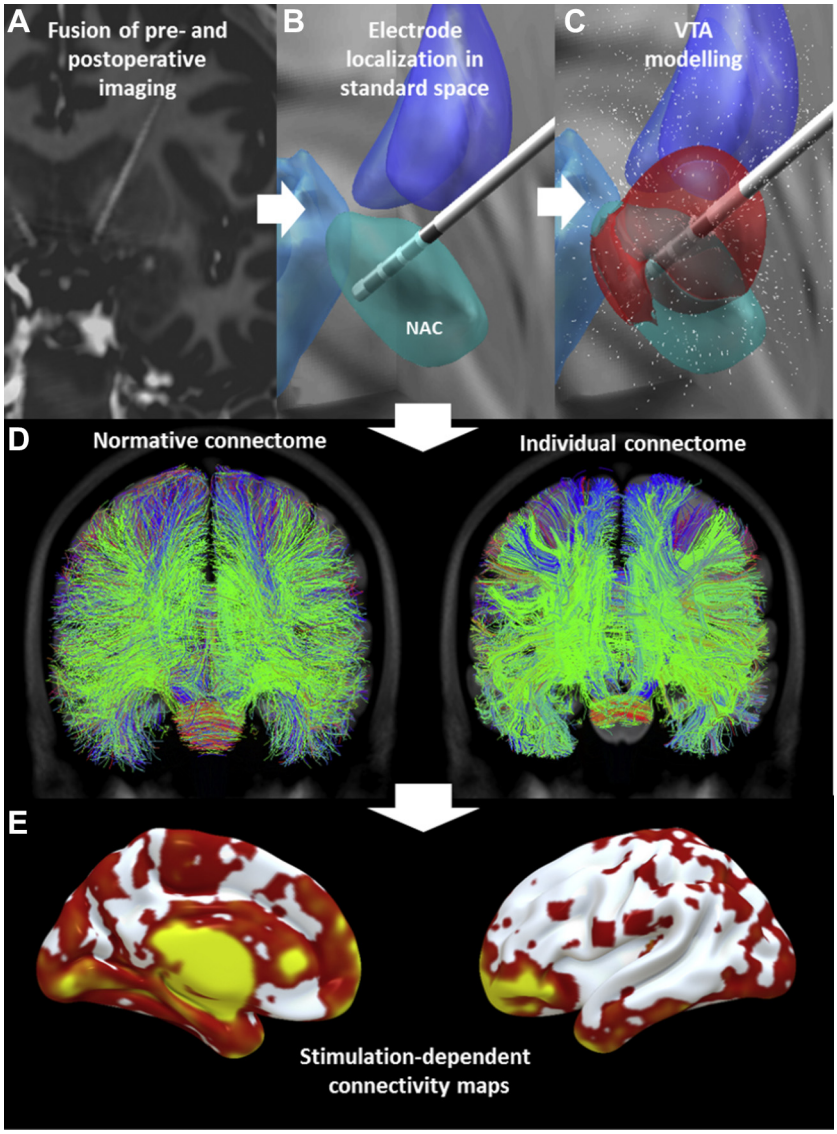

Figure 1. Schematic display of methods applied for identifying deep brain stimulation connectivity. Processing steps included fusion of pre- and postoperative imaging **(A)**, localizing deep brain stimulation leads in standard space **(B)**, modeling volumes of tissue activated (VTA) based on individually applied stimulation parameters **(C)**, calculating both normative and (if available) individual structural connectivity from the VTA to the whole brain **(D)**, and isolating and weighting fiber tracts passing the VTA model, resulting in stimulation-dependent connectivity maps **(E)**. NAC, nucleus accumbens.

estimated during VTA calculation. Thus, fibers running through VTA regions where the electric field was high received a higher score than fibers in the peripheral zones of the VTA. Connectivity strength was then expressed as (weighted) numbers of fiber tracts between stimulation sites and each brain voxel. In a second step, across the group of patients, each voxel on the resulting connectivity maps was then correlated with clinical improvement on the Y-BOCS score using Spearman's rank correlation coefficients, leading to R-maps. High *R* values on these maps identify regions to which strong connectivity is associated with good clinical outcome. As described before (11), because tractography maps are generally not normally distributed, they were transformed into a Gaussian distribution following the approach of van Albada and Robinson (18) and lightly smoothed before calculating the R-maps across the group. Owing to the unnormal distribution of dMRI data, displays of cortical R-maps were restricted to positive correlations with outcome. A further subcortical tract-based analysis was performed to show fiber tracts associated with negative outcome as described below.

Crucially, the R-map may be seen as a model for optimal connectivity from the DBS electrode to the rest of the brain, denoting high values for good regions (i.e., regions where a connectivity is associated with good outcome) and low values for the opposite. To be able to make true predictions on a subset of our cohort, the approach (R-map calculation) was performed separately on the 10 patients with patient-specific dMRI available and the 12 patients for whom the high definition of Human Connectome Project normative connectome was used, as in prior work (11,15,19,20). The resulting $R\text{-map}_{10}$ and $R\text{-map}_{12}$ were thus created on approximately half of the cohort using either patient-specific connectivity data or

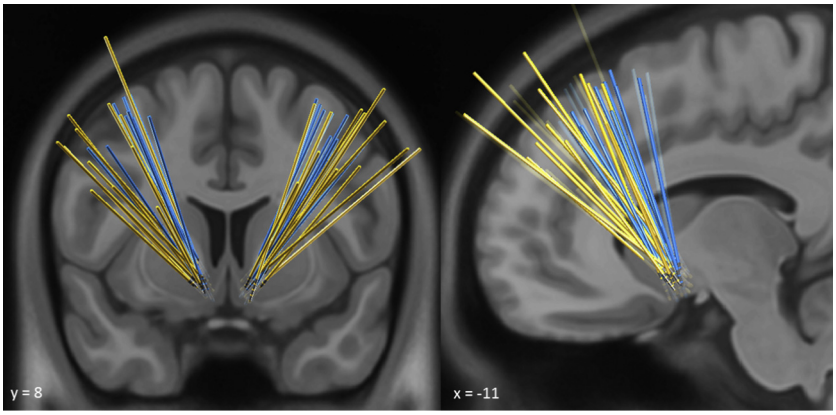

Figure 2. Localization of individual leads. All patients underwent deep brain stimulation surgery to the anterior limb of the internal capsule with the tip of the electrodes located at the posterior border of the nucleus accumbens, receiving two quadripolar deep brain stimulation electrodes. Blue leads represent patients where individual diffusion imaging was available (n = 10), and yellow leads correspond to the remaining patients (n = 12).

normative connectivity data. To test its validity, the R-map$_{10}$ was used to cross-predict outcome of the remaining 12 patients with normative connectivity data and vice versa. To do so, similarity between individual connectivity profiles in one sample and the respective R-map of the other sample was assessed by calculating Fisher z-transformed spatial Spearman correlations fitted to the empirical outcomes using a general linear model (11). This analysis shows how similar each VTA connectivity profile within one sample is to the data-driven optimal connectivity profile of the other sample (defined by the R-map$_{10}$ and R-map$_{12}$) and demonstrates the predictive power of the R-map for out-of-sample data.

After this analysis, an additional R-map$_{22}$ was calculated across the whole group of subjects (with normative connectivity data) to estimate a final optimal connectivity profile informed by as many patients as possible. To validate this map, a leave-one-out cross-validation was applied, where in each step 1 patient was taken out of the model and the empirical outcome was correlated with the predicted outcome derived from the remaining sample.

To further explore whether connectivity to specific cortical regions would be able to explain clinical improvement, we added a region-of-interest (ROI) analysis. This investigated the explanatory value of connectivity estimates from stimulation sites to specific ROIs using the same normative connectivity analysis as on the R-map$_{22}$. ROIs were chosen from prior literature-informed hypotheses (7,8), indicating that effective DBS is associated with involvement of the right MFG and left anterior cingulate cortex. Thus, connectivity between each pair of VTA and right MFG and left anterior cingulate cortex [derived from the automated anatomical labeling atlas (21)] was correlated with clinical outcome using Spearman correlation. Finally, to extract subcortical streamlines predictive of outcome, fiber tracts connected to VTAs across the group of patients were isolated from the normative connectome and a two-sample t test was fitted for each tract between the Y-BOCS improvement scores corresponding to connected versus unconnected VTAs. Fibers were then colored by t values. For the latter analysis, we added a supplementary analysis of fiber tracts associated with improvement of depressive symptoms as assessed by the Beck Depression Inventory (22) (see Supplement for further description). Ultimately, we verified the fiber tract predictive of positive outcome in the Y-BOCS in a focal VTA-based analysis (see Supplement for further description).

RESULTS

The overall sample consisted of 22 patients (13 female; age = 41.7 ± 12.3 years). Mean Y-BOCS score before surgery was 31.3 ± 4.3. After 12 months, Y-BOCS scores decreased significantly by a mean of 30.4 ± 20.1% ($p < .001$). There was no significant correlation between age at surgery ($r = .127$, $p = .574$) or preoperative baseline symptom severity ($r = -.152$, $p = .499$) with clinical outcome.

DBS Connectivity Analysis

In the data-driven analysis, resulting maps denoted correlation coefficients between connectivity and clinical outcome across the group (R-maps). Such maps were calculated on two independent subsets of patients using patient-specific dMRI data (n = 10; R-map$_{10}$) and normative connectivity data (n = 12; R-map$_{12}$) and were used to cross-predict outcome in the respectively remaining patients. Based on the R-map$_{10}$, we were able to significantly predict outcomes of the normative connectivity sample ($r = .545$, $p = .024$). Inversely, we were able to significantly predict outcomes of patient-specific connectivity profiles using the normative R-map$_{12}$ model ($r = .685$, $p = .011$) (Figure 3).

To define a final model of optimal connectivity informed by as many patients as possible, the same analysis was repeated across the full cohort (all using normative data; R-map$_{22}$) (Figure 4). Similarly, to the cohort-specific maps, a positive correlation between connectivity and clinical outcome resulted for areas involving the medial PFC as well as the bilateral lateral PFC. Verifying the validity of the model, individual outcomes were significantly predicted in a leave-one-out cross-validation ($r = .630$, $p < .001$).

An ROI analysis of normative connectome data of the whole sample revealed, congruent to the R-map$_{22}$, significant correlations between clinical improvement and connectivity to the right MFG ($r = .602$, $p = .002$) (Figure 5). Connectivity to left

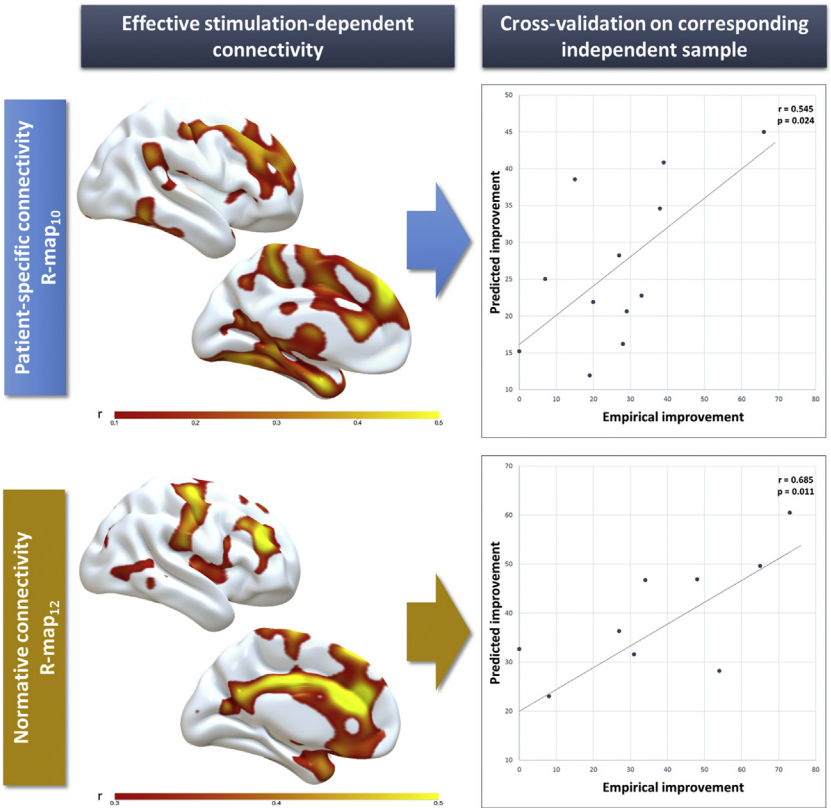

Figure 3. Maps of effective stimulation-dependent connectivity and clinical outcome derived from patient-specific connectomes (blue group [upper row]; R-map$_{10}$, n = 10) and normative connectomes (yellow group [bottom row]; R-map$_{12}$, n = 12) in two independent samples. R values for connectivity to peak voxels were higher than those displayed because the maps were lightly smoothed for visualization (full width at half maximum = isotropic 6 mm). To test validity, we successfully predicted outcome (indicated as % change in the Yale-Brown Obsessive Compulsive Scale) of the respective other sample using the R-map$_{10}$ model (p = .024) and the R-map$_{12}$ model (p = .011).

anterior cingulate cortex did not show a significant relationship with outcome (r = .001, p = .996).

In a final step, fibers predictive of effective DBS connected to VTAs across the whole sample were visualized in a color-coded fashion (Figure 6). This analysis highlighted a clear-cut fiber tract within the ventral ALIC that passes by the ventral striatum, bordering the bed nucleus of the stria terminalis, and connects the middle PFC with the thalamus. Fibers associated with negative outcome encompassed streamlines to the medial forebrain bundle, the posterior limb of the anterior commissure, and fibers within the inferior lateral fascicle. In the VTA-based analysis, the specific fiber bundle within the ALIC was confirmed, showing that VTAs reaching outlined white matter areas apical and posterior of the NAC displayed the highest mean improvement rates (Supplemental Figure S1).

A secondary analysis revealed that fibers encompassing the cingulum, ventromedial PFC, and fornix were associated with improvement of depressive scores (Supplemental Figure S2). Of note, this additional analysis needs to be interpreted with caution because the intervention was not intended to improve depressive symptoms and was performed in only 17 patients with depression scores available.

DISCUSSION

Based on our results, we were able to characterize networks that are associated with and predict reduction of symptoms of severe OCD by ALIC/NAC neuromodulation. We validated the applicability of normative connectome data by significantly cross-predicting outcome of DBS for OCD in two independent data sets consisting of patient-specific and normative connectome data. Furthermore, we calculated a model of optimal stimulation connectivity encompassing the lateral and medial PFC that was able to significantly predict outcome in the overall sample. Within the PFC, our analysis underlined the pivotal role of the right MFG for successful DBS. Finally, we delineated a tractographic target predictive of clinical outcome within the frontothalamic radiation.

Connectivity of Effective Neuromodulation for OCD

We identified a structural network model originating from the stimulation site using both patient-specific (R-map$_{10}$) and normative (R-map$_{12}$) connectomes that is associated with symptom improvement after 1 year of DBS to the ALIC/NAC. Of note, with these models of effective stimulation, we were able to cross-predict outcome in two independent samples based on both patient-specific and normative connectomes. Both networks of beneficial response revealed connectivity to the medial and lateral PFC. In a subsequent analysis, we pooled patients to compute a more powered model of effective DBS. The resulting R-map$_{22}$ showed a positive correlation between connectivity to the bilateral dorsolateral PFCs and the medial prefrontal wall including the cingulate cortex.

This data-driven approach was complemented with an ROI-based approach. Specifically, we wanted to show that

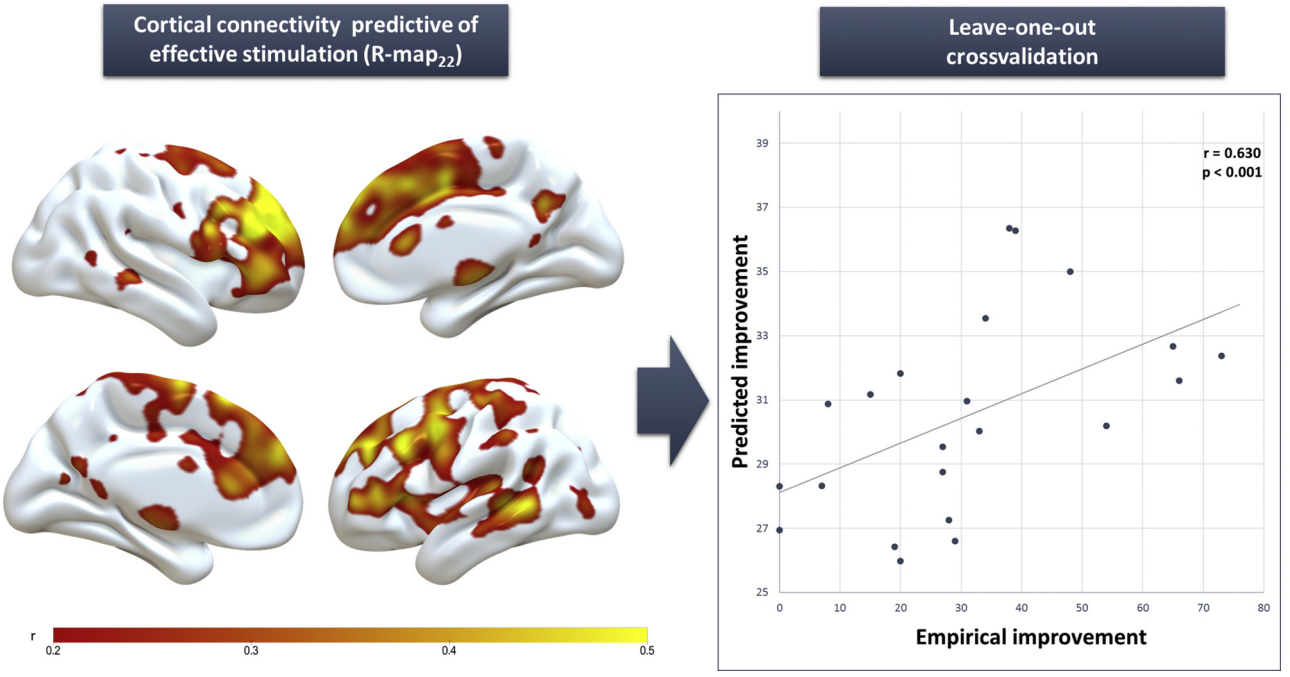

Figure 4. Model of stimulation-dependent connectivity and clinical outcome–derived normative connectomes of the whole sample (R-map$_{22}$, $n = 22$). To test validity of the resulting model of ideal connectivity, we successfully predicted outcomes of individual patients using a leave-one-out design ($r = .630$, $p < .001$), explaining approximately 40% of the variance in clinical improvement (indicated as % change in the Yale-Brown Obsessive Compulsive Scale).

connectivity between stimulation sites and literature-defined cortical regions could explain clinical improvement. This has the potential of using these cortical ROIs in future analyses or studies to, for example, define optimal contacts, surgical targets, or DBS-unrelated analyses. Here, we found a significant positive correlation of outcomes and connectivity to the right MFG. This finding is congruent with the only study (to our knowledge) assessing tractography from DBS stimulation sites in patients with OCD, which found responders to be connected to the right MFG, although this study comprised only 6 patients (8). It is also in line with results of Figee *et al.* (7), who found changes in functional connectivity between stimulation sites

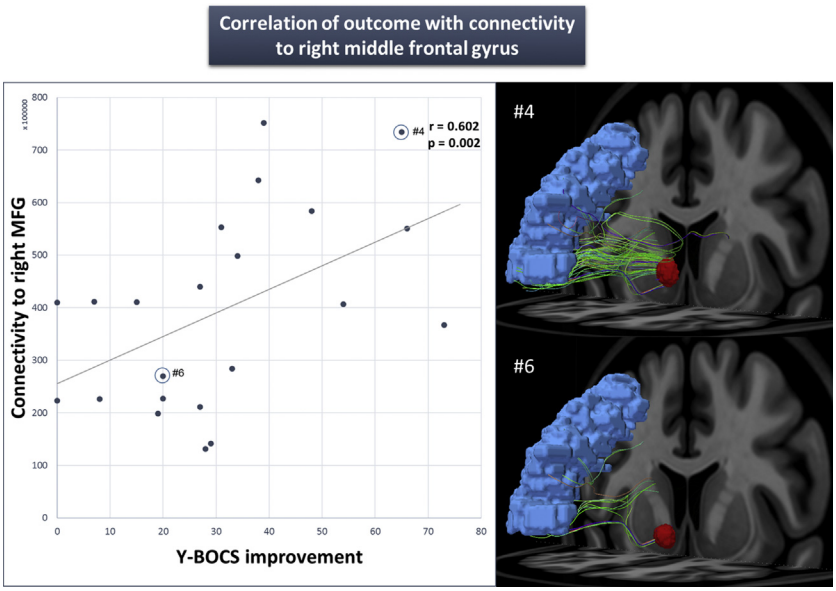

Figure 5. Correlation of outcome and connectivity to region of interest. Connectivity of stimulation sites to the right middle frontal gyrus (MFG) correlated significantly with the outcome of deep brain stimulation after 1 year (indicated as % change in the Yale-Brown Obsessive Compulsive Scale [Y-BOCS]). On the right side, two exemplary patients are displayed. Patient 6 did not respond sufficiently to the intervention and showed relatively sparse connectivity between stimulation site and MFG, whereas patient 4 exhibited enhanced connectivity to the caudal part of the MFG region accompanied by marked improvement in the Y-BOCS.

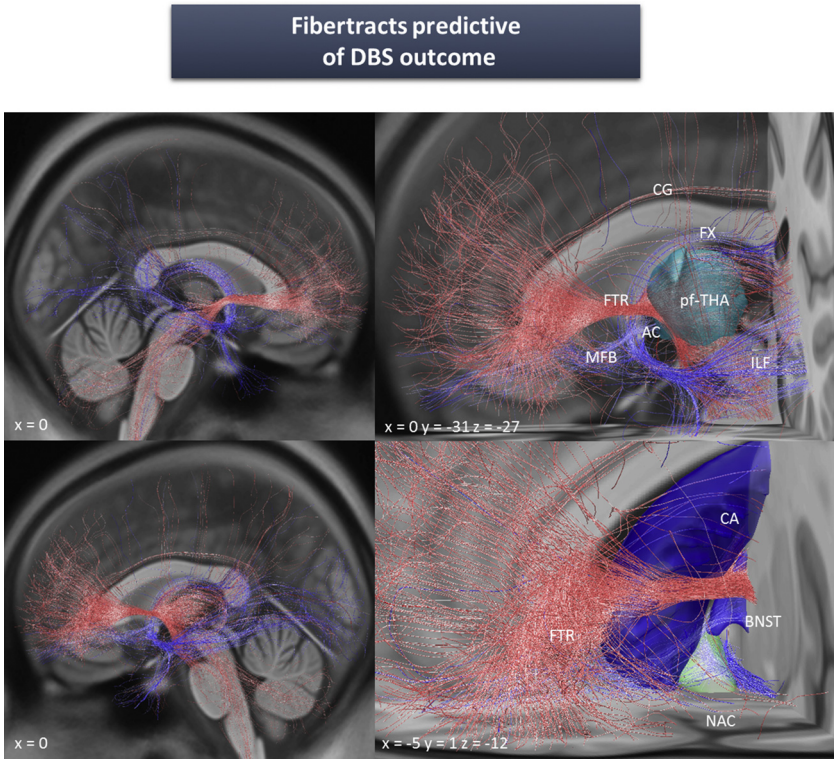

Figure 6. Fiber tracts predictive of positive (red) or negative (blue) clinical outcome when connected to volumes of tissue activated across the group of patients (n = 22). For each fiber tract of the normative connectome, a two-sample t test was fitted between the Yale-Brown Obsessive Compulsive Scale improvements corresponding to connected vs. unconnected volumes of tissue activated. Fibers were then colored by t values. Left panels show a lateral view, and right panels display a close-up view with labeling, highlighting a strong association between connectivity with the anterior frontothalamic radiation (FTR) and clinical response. This effective fiber bundle borders the bed nucleus of the stria terminalis (BNST) and enters the ventral part of the thalamus (cyan) that is connected to the prefrontal cortex (pf-THA). In addition, negative association with more ventrally situated volumes of tissue activated connected to the medial forebrain bundle (MFB) or anterior commissure (AC), whose posterior limb traverses to the temporal cortex, as well as inferior lateral fascicle (ILF) and fornix (FX) becomes evident. CA, nucleus caudatus; CG, cingulum; NAC, nucleus accumbens.

and the right lateral PFC after DBS of the NAC to be significantly correlated with improvement.

In a further analysis of subcortical pathways capable of predicting positive outcome, we identified a clear-cut fiber bundle that channels through the ventral ALIC and connects the middle PFC with the thalamus. This tract was highly discriminative between electrodes that led to optimal versus suboptimal outcomes. The resulting white matter bundle predictive of DBS outcome formed a bottleneck within the ALIC and traversed dorsally to the NAC. Thus, we conclude that the ALIC was a more effective target in our sample, a finding that was shown very recently in Sapap3 mutant mice, the currently predominant OCD animal model (23). This tract is also in line with a study that successfully targeted the bed nucleus of the stria terminalis with DBS (24) and highlights the importance of this structure for research on OCD (25). Very interestingly, the extracted fiber bundle bordered the bed nucleus of the stria terminalis and entered the ventral part of the thalamus at the border of the anterior and inferior thalamic peduncle, with fibers reaching the medial dorsal nucleus and nucleus subthalamicus (Supplemental Figure S3). Thus, this fiber bundle comprises different targets that have been successfully employed for DBS for OCD, suggesting that these different targets form a common network (24,26,27). While connectivity of VTAs with frontothalamic radiation was predictive of response to DBS for OCD, nonresponse was associated with more caudally located VTAs connected to the medial forebrain bundle and anterior commissure. The notion that the ideal target may be located farther away from the currently employed electrode positioning is also supported by the clinical experience that stimulation amplitudes applied in patients with OCD (in our sample a median of 4.7 volts) tend to be higher than those applied in patients with PD or tremor. Hence, adjusting stimulation parameters modulating as many tracts as possible that were associated with good outcome and as few tracts as possible that were associated with poor outcome may improve response and reduce side effects. Regarding our sample, results suggest stimulation of more apical and dorsal contacts with the goal of modulating the frontothalamic radiation within the ALIC. Still, given the small sample size, it is difficult to extract clear clinical recommendations before prospective validation. It may, however, be conceivable that implanted patients who did not respond to DBS may still profit after readjustment of stimulation parameters aiming at capturing the identified specific fiber bundle.

The Connectomic Approach for Predicting DBS Outcome for OCD

In our analysis, we were able to significantly predict outcomes of stimulation-dependent structural connectivity profiles using both a patient-specific model and a normative model of effective connectivity across independent cohorts. Although this cross-validation was performed in a small sample and needs to be interpreted with caution, the same approach could explain 40% of the variance in the whole sample (r = .63, N = 22) in a leave-one-out design. The predictive character of this analysis is all the more relevant because to date there are no robust and conclusive predictors for outcomes of DBS for

OCD, and approximately 40% of patients do not respond to this invasive and costly procedure (4).

The predictive value of connectivity-informed brain stimulation for DBS has already been shown for patients with PD (11). With our results, which comprise the largest OCD sample investigated with such an approach, we add evidence and advocate for investigating the clinical usefulness of such analysis. After careful further validation of our results, it could be worthwhile to determine a patient-specific surgical target based on connectomic analyses depending on preoperative tractography. A similar approach is already practiced in specialized centers for the case of depression (28). Moreover, the technique may be used to guide DBS programming. Based on the patient-specific tractograms of novel patients, suitable stimulation contacts could be proposed by a computer model to facilitate this tedious trial-and-error process.

By validating the patient-specific connectivity models using a normative connectome, we further highlight the utility of such publicly available data. This approach can be helpful in cases where dMRI is not available for a patient and where hyperkinetic disorders render it impossible to acquire a high-quality dMRI scan owing to motion artifacts. As mentioned in Horn *et al.* (11), normative connectomes from healthy subjects have the advantage of large subject numbers, excellent signal-to-noise ratios, and acquisition using specialized MRI hardware designed for connectivity imaging. Such normative connectome data have proven to be valuable in predicting stroke symptoms from patient-specific lesions (20,29,30) and treatment improvement after transcranial magnetic stimulation (31). Another advantage of the normative data is the lack of vulnerability to the low test–retest reliability (32) in dMRI processing pipelines that may form an obstacle to comparing results across centers. In contrast, patient-specific fiber tracts may be advantageous for individual preoperative target selection, bearing in mind individual variances in white matter bundles in the ALIC (33). Our analysis shows that results derived from normative connectomes may be used to predict patients with individualized connectivity data in a split-half design. This does not mean that the information is interchangeable, but it indirectly validates the potential of normative data. The current study would be highly underpowered to estimate whether normative or patient-specific connectivity is better suited to make accurate predictions. We emphasize that both approaches have their advantages and disadvantages for individual patients. Potentially, a combination of both approaches will be a future direction (33). More future work is needed to determine how to best combine the strengths of normative connectomes, patient-based connectomes, and connectivity data from individual patients. Of note, OCD-specific alterations of white matter architecture do not necessarily influence the cross-validation of patient-specific and normative data, given that our approach does not directly compare structural connectivity strength values but rather correlates clinical outcomes with connectivity profiles in each group, thereby blotting out evenly distributed OCD pathologies of quantitative structural connectivity.

A different approach besides the tractographic approach could be to focus on local effects, such as subcortical nuclei, in a purely VTA-based or electrode placement–based analysis. Ultimately, both approaches are linked to each other and should reveal complementary results owing to the neuroanatomical implications. This is also supported by our supplemental VTA-based analysis, which highlights a specific white matter area within the ALIC that matched the fiber bundle in the tractographic analysis.

In the current work, fibers of passage through the stimulation volume were selected and analyzed, a practice that was recently termed activation volume tractography (34). A more elaborate competing method, pathway activation modeling, was introduced in the same article. This method exclusively considers known fiber tracts and estimates activation of those tracts based on the electrode location and stimulation parameters. This analysis is not prone to including false positive tracts (while potentially introducing false negatives). However, a direct transfer from subthalamic DBS to ALIC DBS is not straightforward given that here the tracts with pathophysiological roles have been much less studied than they have been in the subthalamic region for PD. Still, the potential danger of including false positive tracts is specifically relevant because a recent study concluded that the average tractography algorithm results in more false positive tracts than true positive tracts (35). However, we note that precisely in this open competition, the algorithm used in the current study achieved the highest valid connection score among 96 methods. This comparably good ratio of true and false positives thus could be seen as a conservative tractography algorithm that is suitable for clinical connectomics such as the current one.

Conclusions

We were able to identify a network that is associated with and predictive of beneficial effects in DBS for OCD. This network comprised both medial and lateral frontal cortices, in particular the right MFG, merging to an outlined (pre)frontothalamic fiber bundle that passes the striatum within the ventral ALIC. In our sample, increased connectivity of stimulation sites to this fronto-striato-thalamic pathway predicted a large amount of variance in clinical symptom alleviation after 1 year. After further validation, these beneficial connectivity patterns may help to guide both stereotactic surgery and DBS programming in the future. Furthermore, our results may have implications for both cortical and subcortical—and both invasive and noninvasive—neuromodulation protocols.

ACKNOWLEDGMENTS AND DISCLOSURES

This work was supported by the German Research Foundation (Grant No. KFO-219/KU2665/1-2 [to JK] and Grant No. KFO-247 [to AAK]). AH received funding from the Berlin Institute of Health, Professor Klaus Thiemann Foundation, and Stiftung Charité.

We thank Rudolf Nieuwenhuys for his advisory help with neuroanatomical considerations.

JK has received financial support for investigator-initiated trials from Medtronic GmbH. The other authors report no biomedical financial interests or potential conflicts of interest.

ARTICLE INFORMATION

From the Department of Psychiatry and Psychotherapy (JCB, SK, DH, JK) and Department of Stereotactic and Functional Neurosurgery (VV-V), University of Cologne, Max Planck Institute for Metabolism Research Cologne (CM, MT), and Department of Medical Psychology | Neuropsychology and Gender Studies & Center for Neuropsychological Diagnostics and Intervention (AZ), University Hospital Cologne, Cologne; Department of

Neurology (LT), University Hospital Giessen & Marburg, Marburg; Department of Neurology (AAK, AH), Movement Disorders and Neuromodulation Unit, Charité–University Medicine, Berlin; and Department of Psychiatry and Psychotherapy (JK), Johanniter Hospital Oberhausen, Oberhausen, Germany.

AH and JK contributed equally to this work.

Address correspondence to Juan Carlos Baldermann, M.D., Department of Psychiatry and Psychotherapy, University of Cologne, Kerpener Strasse 62, 50937 Cologne, Germany; E-mail: juan.baldermann@uk-koeln.de.

Received Aug 13, 2018; revised Nov 29, 2018; accepted Dec 17, 2018.

Supplementary material cited in this article is available online at https://doi.org/10.1016/j.biopsych.2018.12.019.

REFERENCES

1. Ruscio AM, Stein DJ, Chiu WT, Kessler RC (2010): The epidemiology of obsessive-compulsive disorder in the National Comorbidity Survey Replication. Mol Psychiatry 15:53–63.
2. Ahmari SE, Spellman T, Douglass NL, Kheirbek MA, Simpson HB, Deisseroth K, *et al.* (2013): Repeated cortico-striatal stimulation generates persistent OCD-like behavior. Science 340:1234–1239.
3. Abe Y, Sakai Y, Nishida S, Nakamae T, Yamada K, Fukui K, Narumoto J (2015): Hyper-influence of the orbitofrontal cortex over the ventral striatum in obsessive-compulsive disorder. Eur Neuropsychopharmacol 25:1898–1905.
4. Alonso P, Cuadras D, Gabriëls L, Denys D, Goodman W, Greenberg BD, *et al.* (2015): Deep brain stimulation for obsessive-compulsive disorder: A meta-analysis of treatment outcome and predictors of response. PLoS One 10:e133591.
5. Kohl S, Schönherr DM, Luigjes J, Denys D, Mueller UJ, Lenartz D, *et al.* (2014): Deep brain stimulation for treatment-refractory obsessive compulsive disorder: A systematic review. BMC Psychiatry 14:214.
6. Bourne SK, Eckhardt CA, Sheth SA, Eskandar EN (2012): Mechanisms of deep brain stimulation for obsessive compulsive disorder: Effects upon cells and circuits. Front Integr Neurosci 6:29.
7. Figee M, Luigjes J, Smolders R, Valencia-Alfonso CE, Van Wingen G, De Kwaasteniet B, *et al.* (2013): Deep brain stimulation restores frontostriatal network activity in obsessive-compulsive disorder. Nat Neurosci 16:386–387.
8. Hartmann CJ, Lujan JL, Chaturvedi A, Goodman WK, Okun MS, McIntyre CC, Haq IU (2016): Tractography activation patterns in dorsolateral prefrontal cortex suggest better clinical responses in OCD DBS. Front Neurosci 9:519.
9. Zhou D-D, Wang W, Wang G-M, Li D-Q, Kuang L (2017): An updated meta-analysis: Short-term therapeutic effects of repeated transcranial magnetic stimulation in treating obsessive-compulsive disorder. J Affect Disord 215:187–196.
10. Fox MD, Buckner RL, Liu H, Chakravarty MM, Lozano AM, Pascual-Leone A (2014): Resting-state networks link invasive and noninvasive brain stimulation across diverse psychiatric and neurological diseases. Proc Natl Acad Sci U S A 111:E4367–E4375.
11. Horn A, Reich M, Vorwerk J, Li N, Wenzel G, Fang Q, *et al.* (2017): Connectivity predicts deep brain stimulation outcome in Parkinson disease. Ann Neurol 82:67–78.
12. Avants BB, Tustison N, Song G (2009): Advanced Normalization Tools (ANTS). Insight J (July–December) 1–35.
13. Yeh FC, Tseng WYI (2011): NTU-90: A high angular resolution brain atlas constructed by q-space diffeomorphic reconstruction. NeuroImage 58:91–99.
14. Yeh FC, Verstynen TD, Wang Y, Fernández-Miranda JC, Tseng WYI (2013): Deterministic diffusion fiber tracking improved by quantitative anisotropy. PLoS One 8:e80713.
15. Horn A, Neumann WJ, Degen K, Schneider GH, Kühn AA (2017): Toward an electrophysiological "sweet spot" for deep brain stimulation in the subthalamic nucleus. Hum Brain Mapp 38: 3377–3390.
16. Horn A, Ostwald D, Reisert M, Blankenburg F (2014): The structural-functional connectome and the default mode network of the human brain. NeuroImage 102:142–151.
17. Setsompop K, Kimmlingen R, Eberlein E, Witzel T, Cohen-Adad J, McNab JA, *et al.* (2013): Pushing the limits of in vivo diffusion MRI for the Human Connectome Project. NeuroImage 80:220–233.
18. van Albada SJ, Robinson PA (2007): Transformation of arbitrary distributions to the normal distribution with application to EEG test-retest reliability. J Neurosci Methods 161:205–211.
19. Ewert S, Plettig P, Li N, Chakravarty MM, Collins DL, Herrington TM, *et al.* (2018): Toward defining deep brain stimulation targets in MNI space: A subcortical atlas based on multimodal MRI, histology and structural connectivity. NeuroImage 170:271–282.
20. Darby RR, Horn A, Cushman F, Fox MD (2017): Lesion network localization of criminal behavior. Proc Natl Acad Sci U S A 115:601–606.
21. Tzourio-Mazoyer N, Landeau B, Papathanassiou D, Crivello F, Etard O, Delcroix N, *et al.* (2002): Automated anatomical labeling of activations in SPM using a macroscopic anatomical parcellation of the MNI MRI single-subject brain. NeuroImage 15:273–289.
22. Hautzinger M, Bailer M, H. W&, Keller F (1994): Beck-Depressions-Inventar (BDI): Bearbeitung der deutschen Ausgabe. Bern, Switzerland: Huber.
23. Pinhal CM, van den Boom BJG, Santana-Kragelund F, Fellinger L, Bech P, Hamelink R, *et al.* (2018): Differential effects of deep-brain stimulation of the internal capsule and the striatum on excessive grooming in Sapap3 mutant mice. Biol Psychiatry 84:917–925.
24. Luyten L, Hendrickx S, Raymaekers S, Gabriëls L, Nuttin B (2016): Electrical stimulation in the bed nucleus of the stria terminalis alleviates severe obsessive-compulsive disorder. Mol Psychiatry 21:1272–1280.
25. Kohl S, Baldermann JC, Kuhn J (2016): The bed nucleus: A future hot spot in obsessive compulsive disorder research. Mol Psychiatry 21:990–991.
26. Jiménez F, Nicolini H, Lozano AM, Piedimonte F, Salín R, Velasco F (2013): Electrical stimulation of the inferior thalamic peduncle in the treatment of major depression and obsessive compulsive disorders. World Neurosurg 80:S30.e17–S30.e25.
27. Mallet L, Polosan M, Jaafari N, Baup N, Welter M-L, Fontaine D, *et al.* (2008): Subthalamic nucleus stimulation in severe obsessive-compulsive disorder. N Engl J Med 359:2121–2134.
28. Noecker AM, Choi KS, Riva-Posse P, Gross RE, Mayberg HS, McIntyre CC (2018): StimVision software: Examples and applications in subcallosal cingulate deep brain stimulation for depression. Neuromodulation 21:191–196.
29. Joutsa J, Horn A, Hsu J, Fox MD (2018): Localizing parkinsonism based on focal brain lesions. Brain 141:2445–2456.
30. Joutsa J, Shih LC, Horn A, Reich MM, Wu O, Rost NS, Fox MD (2018): Identifying therapeutic targets from spontaneous beneficial brain lesions. Ann Neurol 84:153–157.
31. Whitwell JL, Shiung MM, Przybelski SA, Weigand SD, Knopman DS, Boeve BF, *et al.* (2008): MRI patterns of atrophy associated with progression to AD in amnestic mild cognitive impairment. Neurology 70:512–520.
32. Petersen MV, Lund TE, Sunde N, Frandsen J, Rosendal F, Juul N, Østergaard K (2017): Probabilistic versus deterministic tractography for delineation of the cortico-subthalamic hyperdirect pathway in patients with Parkinson disease selected for deep brain stimulation. J Neurosurg 126:1657–1668.
33. Nanda P, Banks GP, Pathak YJ, Sheth SA (2017): Connectivity-based parcellation of the anterior limb of the internal capsule. Hum Brain Mapp 38:6107–6117.
34. Gunalan K, Chaturvedi A, Howell B, Duchin Y, Lempka SF, Patriat R, *et al.* (2017): Creating and parameterizing patient-specific deep brain stimulation pathway-activation models using the hyperdirect pathway as an example. PLoS One 12:176132.
35. Maier-Hein KH, Neher PF, Houde J-C, Côté M-A, Garyfallidis E, Zhong J, *et al.* (2017): The challenge of mapping the human connectome based on diffusion tractography. Nat Commun 8:1349.